



Specific ion effects on the properties of cationic Gemini surfactant monolayers

T. Alejo, M.D. Merchán, M.M. Velázquez*

Departamento de Química Física, Facultad de Ciencias Químicas, Universidad de Salamanca, 37008 Salamanca, Spain

ARTICLE INFO

Article history:

Received 12 July 2010

Received in revised form 3 March 2011

Accepted 9 March 2011

Available online 22 March 2011

Keywords:

Cationic Gemini surfactant

Langmuir monolayers

Langmuir–Blodgett films

Hofmeister effect

Atomic force microscopy

Brewster angle microscopy

ABSTRACT

The effects of some anions of the Hofmeister series and different divalent cations of alkaline earth metals on the properties of Langmuir monolayers of the cationic Gemini surfactant ethyl-bis (dimethyl octadecylammonium bromide) have been investigated. Surface pressure and potential isotherms at the air–water interface were obtained on aqueous subphases containing sodium salts with several anions of the Hofmeister series (Cl^- , NO_3^- , Br^- , I^- , ClO_4^- , and SCN^-). The influence of the investigated anions on the monolayer properties can be ordered according to the Hofmeister series with a change in the order between bromide and nitrate anions. On the other hand, for a given anion, the cation of the salt also influences the surface properties of the Langmuir films. The monolayers can be transferred onto mica by the Langmuir–Blodgett technique and then the Langmuir–Blodgett films were characterized by atomic force microscopy (AFM). The AFM images show that the molecules become more closely packed and nearly vertical to the surface when anions screen the electric charge of the surfactant molecules.

© 2011 Elsevier B.V. All rights reserved.

1. Introduction

Recently, studies of surface properties of simple electrolyte have renewed attention because they play a key role in the surface chemistry of the atmosphere aerosol [1] as well as in many areas of the Physical Chemistry such as electrochemistry, catalysis, drug availability or ion separation [2].

The first studies of surface properties of simple electrolytes dealt with thermodynamic properties and they indicated that the surfaces are formed by an ion-free water layer [3]. In contrast, the most recent experiments using vibrational sum frequency spectroscopy (VSFG) [4–6] along with molecular dynamic simulations [7–9] show that large polarizable anions reside in the surface region. The VSFG measurements also showed that the divalent counter-cations of salts play an important role concerning to the propensity of anions for the air–water interface [10,11]. This fact raises some important questions related to interactions between ions present in the subphase and molecules adsorbed at the interface. These interactions are of major importance in the manufacture of high-quality Langmuir–Blodgett films (LB films) with potential applications in thin film technology [12]. One of the main difficulties in building materials for molecular electronic is that high intermolecular organization is necessary to achieve the desired properties. One possible approach to create such molecular order is amphiphilic self-assembly into a monolayer on saline aqueous subphases followed by Langmuir–Blodgett transfer. Thus, when ions are present in the subphase, the

surfactant monolayer usually becomes more ordered [13] and transfers more easily to solid substrates (LB films) [14]. Aggregates with different structure have been observed in monolayers prepared on subphases containing divalent ions [15,16]. These self-assembly systems are interesting from the fundamental point of view [17] and from technological applications [18,19].

In order to gain insights in the effects of specific interactions between anions and surfactants on the structure and properties of Langmuir and LB films of surfactants, we study the effects of different anions of the Hofmeister series on both the Langmuir and the LB films of the cationic Gemini surfactant ethyl-bis (dimethyl octadecylammonium bromide), abbreviated as 18-2-18. We also study the effect of divalent cations in the gradient concentration of anions near the surface. We chose the cationic surfactant 18-2-18 because Gemini surfactants provide a high surface activity relative to the corresponding monocationary surfactants [20] and can be used as templates for preparation of nanomaterials [21]. The behavior of water-soluble Gemini surfactants in solutions and at the air–water interface has been thoroughly investigated and an interesting review of results was carried out by Zana [22]; however, the properties of Gemini insoluble monolayers have received less attention [23–28] although they are promising candidate as component in technological applications such as energy-storage or liquid-crystal devices.

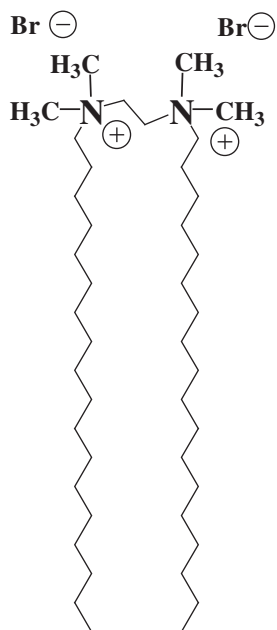
2. Materials and methods

2.1. Materials

Gemini surfactant 18-2-18, Scheme 1, was synthesized using the method described by Zana et al. [29] with some significant modifications

* Corresponding author at: Departamento de Química Física, Facultad de Ciencias Químicas, Universidad de Salamanca, Plaza de los Caídos s/n, 37008 Salamanca, Spain. Fax: +34 923294500x1547.

E-mail address: mvsal@usal.es (M.M. Velázquez).



Scheme 1. Molecular structure of the cationic Gemini surfactant ethyl-bis (dimethyl octadecylammonium bromide), abbreviated as 18-2-18.

introduced in order to improve the purity of the product. Modifications introduced are recrystallization of the product from mixtures of chloroform and acetonitrile, and purification by column chromatography (silica gel, eluent: acetone and methanol). The product was characterized by mass spectrometry and nuclear magnetic resonance to guarantee a degree of purity >99.9%, necessary for the correct interpretation of surface experiments.

Chloroform (PAI, filtered) used to prepare the spreading solutions was from Sigma-Aldrich. Millipore Ultra pure water prepared using a combination of RiOs and Milli-Q systems from Millipore was used to prepare the saline subphases. The salts of high purity were purchased from Sigma-Aldrich and baked for 48 h at 300–500 °C to remove traces of organic compounds. The salt concentration dissolved in the subphase ranged from 0.01 M to 1 M. The LB substrate muscovite (mica) quality V-1 was supplied by EMS (USA). The mica surface was freshly cleaved before use.

2.2. Preparation of Langmuir monolayers and Langmuir–Blodgett films

The surface pressure measurements were performed on two computer-controlled Teflon Langmuir film balances, Minitrough and Standard KSV2000-2 (KSV, Finland). The surface pressure was measured with a Pt-Wilhelmy plate connected to an electrobalance. The temperature is controlled by flowing thermostated water through jackets at the bottom of the trough. The water temperature was maintained by means of the thermostat/cryostat Lauda Ecoline RE-106. The temperature near the surface was measured with a calibrated sensor from KSV.

In order to confirm the stability of the monolayer, two different forms for preparing the monolayers were used. In the first one the surface concentration was changed by subsequent additions of the surfactant solutions on the liquid/air interface using a micrometer Hamilton syringe. The syringe precision is 1 μL . The surface pressure was continuously monitored, and the equilibrium value was taken when the surface pressure remained constant for at least 10 min. In the second way, the monolayers were symmetrically compressed by moving two barriers under computer control after the spreading of the surfactant solution. The compression rate was 5 mm/min. The spreading solutions of concentration around 5×10^{-4} M were prepared on chloroform by weight using an analytical balance precise to 0.01 mg.

A KSV2000 System 2 for LB deposition was also used. The monolayer was transferred to the solid substrate by symmetric compression at barriers speed of 5 mm/min, with the substrate into the trough by vertically dipping it at 5 mm/min.

2.3. Surface potential measurements

The surface potential ΔV was measured in the Teflon Langmuir Minitrough (KSV, Finland). A Kelvin probe KSVSPOT from KSV located approximately 2 mm above the aqueous surface was used. KSVSPOT is based on the non-contact vibrating plate capacitor method with the reference electrode placed in the subphase. The surface potential of monolayers was determined relative to the surface potential of the supporting electrolyte and of water if no salt was added to the subphase. Each reported value is an average over five measurements and the standard deviation of these measurements was considered the experimental error.

2.4. Brewster angle microscopy (BAM)

The morphology of Gemini surfactant layers at the air–water interface was observed using a Brewster angle microscope BAM (Optrel BAM 3000 from KSV) mounted on the Teflon Langmuir trough through Standard KSV2000-2 (KSV, Finland). The microscope uses a helium–neon laser of 10 mW (632.8 nm) and a digital camera model Kam Pro-02 (768 \times 494 pixels) from EHD.

2.5. Atomic force microscopy (AFM)

AFM images of the LB films of 18-2-18 on mica substrates were obtained in constant repulsive force mode by AFM (Nanotec Dulcinea, Spain) with a rectangular microfabricated silicon nitride cantilever (Olympus OMCL-RC800PSA) with a height of 100 μm , a Si pyramidal tip and a spring constant of 0.73 N/m. The scanning frequencies were usually in the range between 0.5 and 2.0 Hz per line. The measurements were carried out under ambient laboratory conditions.

3. Results and discussion

3.1. Characterization of 18-2-18 monolayer at the air/water interface

The surface pressure–molecular area isotherms were performed at 293 K, under the desorption temperature, $T_d = 302$ K [30]. The pressure–area isotherms obtained by subsequent additions and symmetric compression for monolayers on water subphase are represented in Fig. 1a. As can be observed the isotherms agree with each other until the monolayer collapse. Above this pressure, the surface pressure of the monolayer obtained by compression is higher than that obtained by addition. Similar behavior was observed in monolayers on saline subphases. Because we are not interested in study states corresponding to monolayers collapsed we obtained the rest of the isotherms by symmetric compression.

The monolayers can exist in different states that can be determined in terms of the equilibrium elasticity modulus [31]. According to it, we calculate the equilibrium elasticity modulus of the 18-2-18 monolayer on water subphase from the pressure isotherms

and the equation: $\epsilon_0 = \Gamma \left(\frac{\delta \pi}{\delta \Gamma} \right)_T$. Results are represented in Fig. 1b and

show that for molecular areas above 200 \AA^2 the elasticity modulus, ϵ_0 , gets a very small value characteristic of gas phase. BAM images in this region show different domains which are seen as stripes and circles, see Fig. 1d, and which disappear when the surface pressure increases, Fig. 1c. Hence, the region with low ϵ_0 values was ascribed to a gas–liquid expanded phase coexistence region.

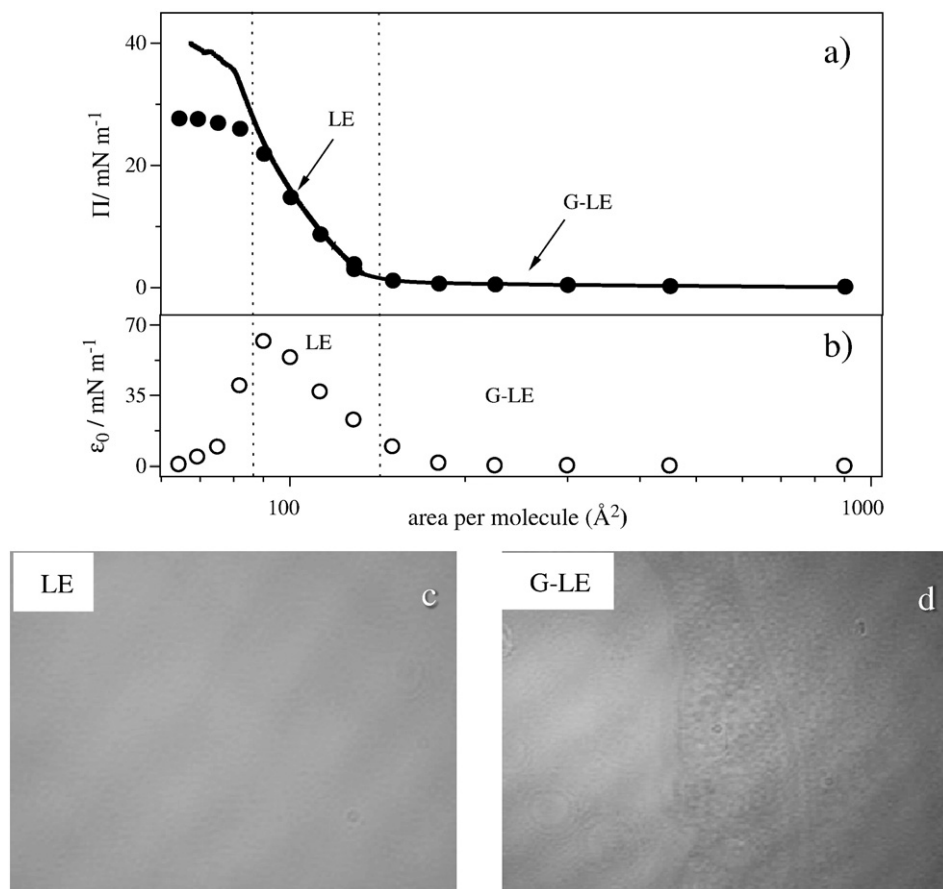


Fig. 1. Surface pressure isotherms (a) obtained by addition (solid circles) and by symmetric compression (line) at 293 K. (b) Variation of the equilibrium elasticity with the surfactant surface concentration. BAM images corresponding to: (c) LE and (d) G-LE. Image size: 350 × 270 μm. The arrows in the isotherm point to the monolayers observed by BAM.

The equilibrium elasticity modulus values from the liftoff to the onset of the collapse film are characteristic of liquid-expanded (LE) phase, indicating that during compression before the collapse the phase condensed does not appear. This fact was previously observed for monolayers of bis (quaternary ammonium bromide) surfactants with spacers larger than the one used in this work [27].

3.2. Characterization of 18-2-18 monolayer on saline subphases

In order to gain insights in the effect of saline subphases on the properties of 18-2-18 monolayers, we study the effect of different anions of the Hofmeister series dissolved in the subphase on the properties of the surfactant monolayer. Firstly, we study the salt concentration effects in the monolayer. Fig. 2 shows results for Gemini monolayers on NaBr aqueous subphases. As can be seen in Fig. 2 the area per molecule decreases rapidly with increasing salt concentration and it remains constant above 0.1 M of NaBr. Similar trend was observed for other salts. It is well established that the molecular area of surfactants in monolayers is related to the balance between repulsions and attractions. According to it, when the electric charge of ionic surfactant is screened, the repulsions between the surfactant molecules decrease and monolayers become more compressed. Therefore, from our results it is possible to conclude that the addition of salts screens the surfactant and consequently the monolayer becomes more compressed. To study the effect of anions of the Hofmeister series, the anion concentration dissolved in the subphase was kept constant in 0.20 M, using this concentration the surfactant molecules at the interface are in their most compressed state. Fig. 3 shows the isotherms corresponding to monolayers on subphases containing sodium salts of different anions. The isotherms in Fig. 3

were obtained at 293 K. The morphology of the isotherm is quite similar to the isotherm on water subphase; however, it becomes more compressed according to the following order: water < Cl⁻ < NO₃⁻ < Br⁻ < I⁻ < ClO₄⁻ < SCN⁻. The equilibrium elasticity values were used to identify the different states of the monolayers. The values found show that before the collapse the phase condensed does not appear. This behavior is similar to that observed for the monolayer on water subphase. Fig. 4 shows the BAM images in the gas-liquid expanded (G-LE) regions for monolayers on subphases with different salts. If we

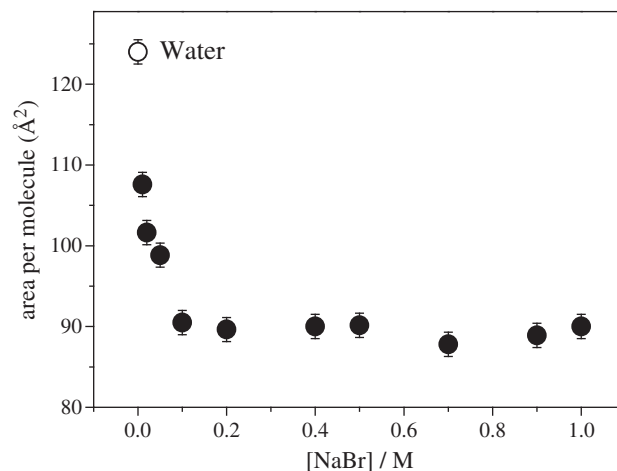


Fig. 2. Variation of the surfactant molecular area with the NaBr concentration dissolved in the aqueous subphase.

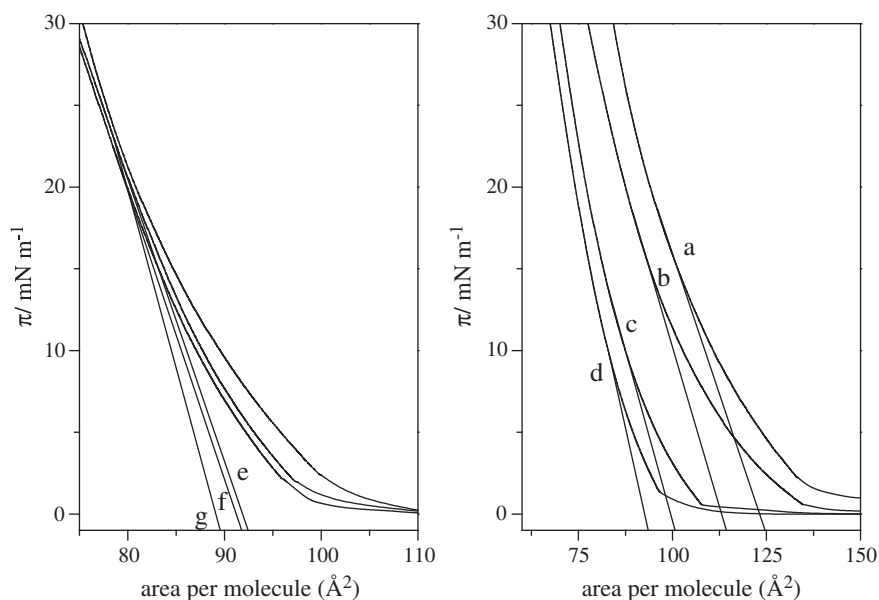


Fig. 3. Surface pressure isotherms obtained for Langmuir monolayers of 18-2-18 on subphases containing 0.20 M of the indicated anions: a) water, b) chloride, c) nitrate, d) bromide, e) iodide, f) perchlorate and g) thiocyanate. The counter-cation was always Na^+ .

compare these images with those corresponding to the same region for the monolayer on water, Fig. 1d, it is possible to conclude that the morphology of domains is quite similar. As it happens in monolayers on water, Fig. 1c, BAM images for LE monolayers on saline subphases do not present aggregates (not shown).

The area per molecule extrapolated to zero surface pressure and the maximum equilibrium elasticity values for the LE state are collected in Table 1. For comparative purposes the table also presents the corresponding values for the monolayer on water subphase. The area per molecule for the monolayer on water is 124 \AA^2 . This value is consistent with the molecular area for the same Gemini surfactant with 3 methylene groups as spacer, 18-3-18, (1.28 nm^2) [28]. In monolayers

prepared on saline subphases the area per molecule decreases according to the series: $\text{water} < \text{Cl}^- < \text{NO}_3^- < \text{Br}^- < \text{I}^- < \text{ClO}_4^- < \text{SCN}^-$, and the maximum value of the equilibrium elasticity modulus increases in the same order. These facts can be attributed to the screening of the surfactant electric charge by electrolytes dissolved in the subphase. Thus, when the electric charge of the surfactant adsorbed at the interface is screened the repulsions between molecules decrease and the monolayers become more compressed, increasing the chain packing and the elasticity of the monolayer. Additional information about the influence of anions on monolayers of 18-2-18 was obtained by means of surface potential measurements. For the sake of clarity, we represent only some surface potential isotherms in Fig. 5.

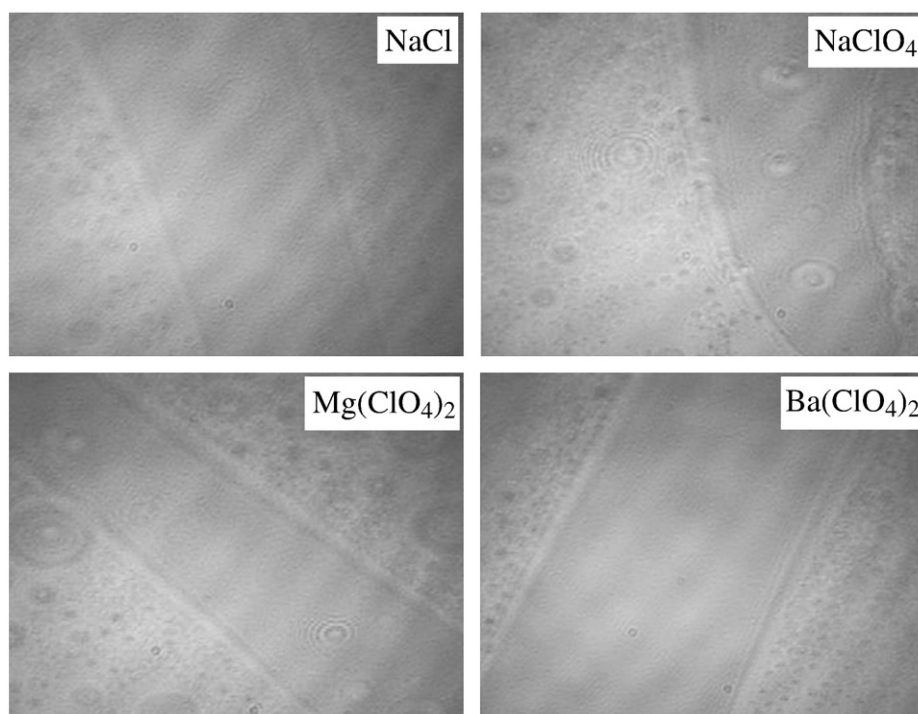


Fig. 4. BAM images of G-LE regions of 18-2-18 on different saline subphases. Image size: $350 \times 270 \mu\text{m}$.

Table 1

Maximum equilibrium elasticity modulus and area per molecule values for 18-2-18 LE monolayers on different subphases.

| Subphase | $\epsilon_{\max}/\text{mN m}^{-1}$ | Area per molecule (\AA^2) |
|--------------------|------------------------------------|--------------------------------------|
| Water | 60 | 124 |
| NaCl | 75 | 113 |
| NaNO ₃ | 85 | 100 |
| NaBr | 85 | 93 |
| NaI | 100 | 92 |
| NaClO ₄ | 110 | 91 |
| NaSCN | 120 | 89 |

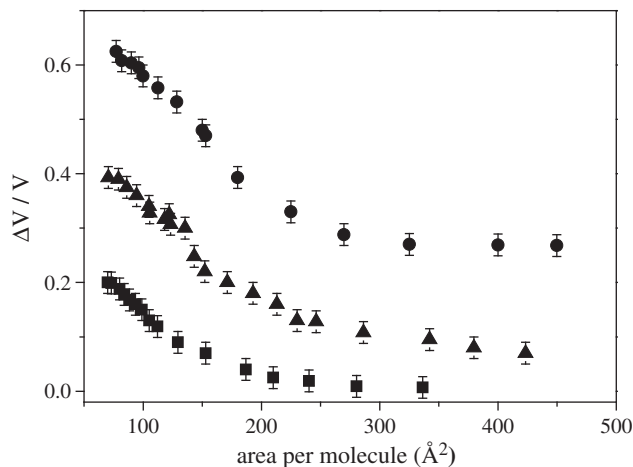


Fig. 5. Surface potential isotherms at 293 K of 18-2-18 monolayers prepared on different subphases: (circles) water; (triangles) 0.20 M NaCl and (squares) 0.20 M NaClO₄.

Results in Fig. 5 show that the surface potential values are always positive as correspond to a monolayer containing cationic surfactant molecules. In addition, the surface potential at a given area decreases with the salt concentration dissolved in the subphase indicating that anions compensate the charges of the surfactant molecules. The surface potential values for a given surface area follows the order: water < Cl⁻ < NO₃⁻ < Br⁻ < I⁻ < ClO₄⁻ < SCN⁻. All these results indicate that anions have different ability to compensate the electric charge of the surfactant. This behavior is consistent with the specific ion effects observed in other cationic monolayers [32]. Other specific anion effects have been observed in the properties of monolayers of the zwitterionic surfactants [33–35].

From all these results, we can conclude that the effect of the addition of salts to the aqueous subphase on the equilibrium properties of surfactant monolayers depends on the ability of the anions to compensate the electric charge of the surfactant adsorbed at the air–water interface. Our results demonstrate that the ability of anions to screen the electric charge of the Gemini surfactant increases in the order: Cl⁻ < NO₃⁻ < Br⁻ < I⁻ < ClO₄⁻ < SCN⁻. This ordering is a Hofmeister series, Scheme 2, with a change in the order between bromide and nitrate anions. The Hofmeister series was established to ordering anions based on their ability to salt-out proteins from aqueous solutions [36]. It is also known that a variety of processes such as solubility of salts, zeta potential, electrolyte activities, critical micellar concentrations, colloidal stability, etc., follow this series [37]. More recently, theoretical [7–9] and experimental results [4–6] have illustrated the influence of the Hofmeister series on the propensity of

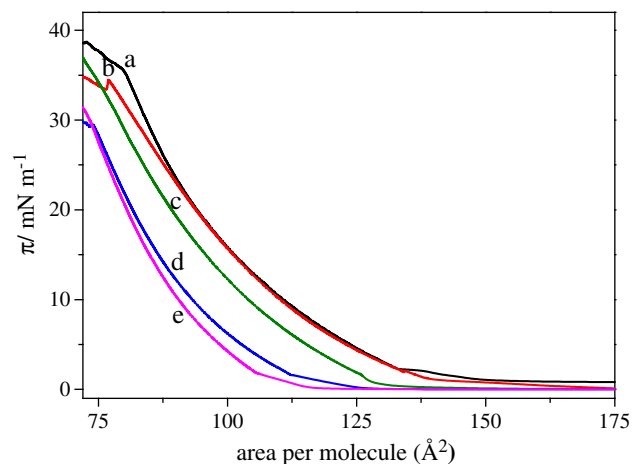


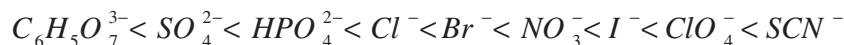
Fig. 6. Surface pressure isotherms for Langmuir monolayers of 18-2-18 on subphases containing different nitrate salts of different divalent cations: a) water, b) magnesium, c) calcium, d) strontium and e) barium. The salt concentration in the subphases remains constant in 0.10 M.

anions for the air–water interface. The experiments using VSFG [4] and normalized second harmonic generation spectroscopy (SHG) [38] indicated that the propensity of anions for the interface increases as the Hofmeister series. On the other hand VSFG measurements have also demonstrated the presence of NO₃⁻ at the interface [10,11]. The fact that the nitrate symmetric stretch can be observed by VSFG is signature of structural changes on the NO₃⁻ adsorbed at the interface because the symmetric stretch of the planar structure of NO₃⁻ in bulk, D_{3h} symmetry, is not VSFG active [10]. The structural change on the nitrate anions at the interface could be responsible of the observed inversion in the order between bromide and nitrate anions [37].

Vibrational sum frequency spectroscopy also showed that the divalent counter-cations play an important role concerning to the propensity of anions for the air–water interface [10,11]. Therefore, we study the effect of the addition of different divalent cations in the subphase on the equilibrium properties of 18-2-18 monolayers.

Fig. 6 shows the surface pressure–molecular area isotherms for the Gemini surfactant monolayers on subphases containing different nitrate salts of the divalent cations; the salt concentration is always 0.10 M.

As can be observed in the figure, the isotherms shift to lower areas per molecule as the cation size increases. The area per molecule extrapolated to zero surface pressure in the LE region and the maximum of the equilibrium elasticity modulus values are collected in Table 2. For the sake of comparison Table 2 also presents the values obtained for different perchlorate salts of divalent cations. Results in Table 2 clearly demonstrate that the monolayer becomes more compressed according to the following order Mg²⁺ < Ca²⁺ < Sr²⁺ < Ba²⁺. The elasticity increases in a similar way to the decrease of the molecular area of surfactant molecules at the interface. In addition, the surface potential at a given molecular area decreases following the same order (not shown). All these results indicate that the electric charge of monolayers of the Gemini surfactant is screened following the series: Mg²⁺ < Ca²⁺ < Sr²⁺ < Ba²⁺. This behavior shows the important role that the counter-cation plays in the propensity of a given anion for the air–water interface and it is consistent with theoretical [39] and experimental [10,11] results concerning to the effects of cations on the structure of air–aqueous interface.



Scheme 2. The Hofmeister series of anions [36].

Table 2

Maximum equilibrium elasticity modulus and area per molecule values for 18-2-18 LE monolayers on subphases containing different salts.

| Subphase | $\epsilon_{\max}/\text{mN m}^{-1}$ | Area per molecule (\AA^2) | Subphase | $\epsilon_{\max}/\text{mN m}^{-1}$ | Area per molecule (\AA^2) |
|-----------------------------------|------------------------------------|--------------------------------------|------------------------------------|------------------------------------|--------------------------------------|
| Water | 60 | 124 | Water | 60 | 124 |
| Mg(NO ₃) ₂ | 62 | 122 | Mg(ClO ₄) ₂ | 84 | 97 |
| Ca(NO ₃) ₂ | 65 | 115 | Ca(ClO ₄) ₂ | 88 | 94 |
| Sr(NO ₃) ₂ | 68 | 102 | – | – | – |
| Ba(NO ₃) ₂ | 75 | 98 | Ba(ClO ₄) ₂ | 103 | 85 |

3.3. AFM images of the Langmuir–Blodgett films

In order to test the influence of saline subphases on the properties of LB films of the Gemini surfactant 18-2-18, Langmuir films were prepared on water subphases without and with salts and then, were

transferred from the interface onto mica using the Langmuir–Blodgett methodology. The morphology of LB films was observed by AFM. Fig. 7 shows the images and the cross-section profiles of LB films prepared with Langmuir monolayers of 18-2-18 on different subphases at distinct surface pressures. The Fig. 7a presents the image of the LB film constructed from the Langmuir monolayer on water subphase corresponding to the LE state ($\pi = 19 \text{ mN/m}$ and $\Gamma = 1.4 \cdot 10^{-6} \text{ mol/m}^2$). The image shows a film with height around 0.8 nm. This height is lower than the length of the fully extended hydrocarbon chain of 18 methylene groups (2.4 nm) [40], indicating that the surfactant molecules do not stand up at this surface pressure. This behavior is similar to that previously observed for LB films of other Gemini surfactants [28].

We explore the effect of salts dissolved in the subphase on the morphology of LB films by transferring LE Langmuir monolayers on different saline subphases with the same surface concentration of 18-2-18 than the one on water subphase ($\Gamma = 1.4 \cdot 10^{-6} \text{ mol/m}^2$). Fig. 7b

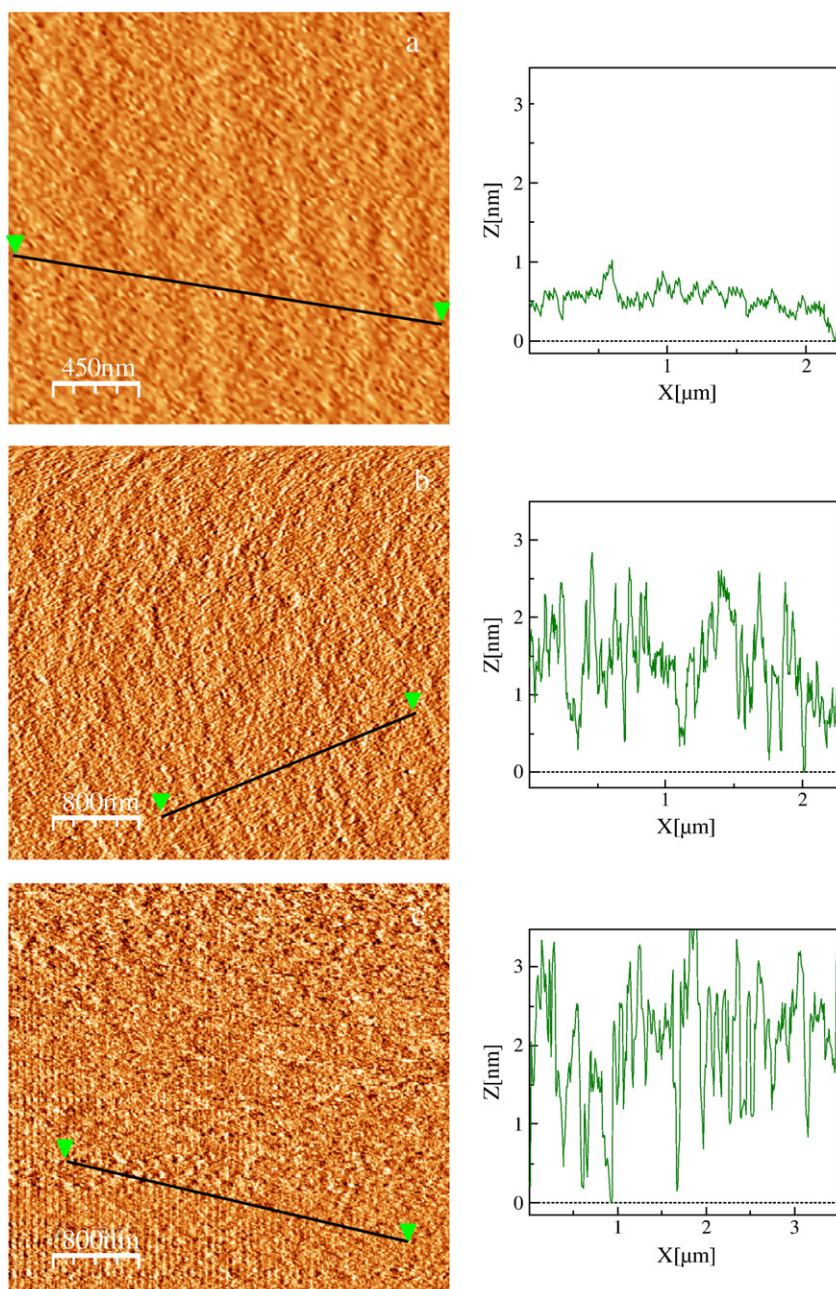


Fig. 7. AFM images of the LB films on mica for different 18-2-18 monolayers: a) on water subphase at surface pressure 19 mN/m; b) on aqueous subphase containing 0.10 M of Ba(NO₃)₂ at surface pressure 10 mN/m and c) on a saline subphase containing 0.10 M of Ba(ClO₄)₂ at 30 mN/m.

presents the AFM image and the cross-section profile of the LB film built on $\text{Ba}(\text{NO}_3)_2$ 0.10 M. The image shows a quasi-homogeneous film of surfactant molecules with height between 2 and 2.5 nm, this thickness is similar to the length of the fully extended chain of the surfactant molecule. Similar trend was observed for the rest of monolayers on saline subphases, to illustrate this fact we present in Fig. 7c the AFM image of a LB film constructed by transferring a concentrated Langmuir film in the LE state ($\Gamma = 2.5 \cdot 10^{-6} \text{ mol/m}^2$) prepared on $\text{Ba}(\text{ClO}_4)_2$ 0.10 M. It is also interesting to notice that below the collapse region even in the most concentrated monolayers we do not detect the formation of micelles at the surface; this behavior is contrary to results found in monolayers of cationic Gemini surfactants with larger spacer than the 18-2-18 surfactant [26].

According to these results, it is possible to conclude that the AFM images of Langmuir–Blodgett films are consistent with the equilibrium properties of the Langmuir monolayers discussed in the first part of this paper. Thus, the AFM images of LB films reveal that the LE monolayers of 18-2-18 become more closely packed and nearly vertical to the surface when the electric charge of the surfactant molecules is efficiently screened by anions dissolved in the aqueous subphase.

4. Conclusions

Anions in the aqueous subphases influence the surface behavior of the cationic Gemini surfactant ethyl-bis (dimethyl octadecylammonium bromide) according to the Hofmeister series with a change in the order between bromide and nitrate anions. On the other hand, for a given anion, the counter-cation also influences the surface properties of the Gemini surfactant films.

The 18-2-18 monolayers can be transferred onto mica using the LB methodology. AFM images of the LB films show that the surfactant molecules become more closely packed and nearly vertical to the surface when the anions screen the electric charge of the surfactant head groups. Finally, it is interesting to notice that, conversely to results obtained for LB films of bis-(quaternary ammonium halide) surfactants with spacers larger than the one used in this work, no micellar aggregates at the interface were detected in 18-2-18 films. This result agrees very well with molecular dynamics simulations carried out by other authors with other Gemini surfactants. Thus, molecular dynamics simulations showed that only surfactants with the shortest spacers ($\leq 3\text{CH}_2$) give stable monolayers while when the length of the spacer increases, several surfactant molecules move from the interface to the primary monolayer below the interface exhibiting aggregate formation [41].

Acknowledgements

The authors thank financial support from ERDF and MEC (MAT 2007–62666) and from Junta de Castilla y León (SA138A08). We also thank Dr. J. Anaya (Departamento de Química Orgánica, Universidad

de Salamanca) for the help in the synthesis of the Gemini surfactant. The authors also acknowledge to Drs. J. J.A. Pérez-Hernández and J. Hernández-Toro and to Ultra-Intense Lasers Pulsed Center of Salamanca (CLPU) for the AFM measurements.

References

- [1] B.J. Finlayson-Pitts Jr., *Science* 276 (1997) 1045.
- [2] A.G. Volkov, D.W. Deamer, D.L. Tanelian, V.S. Markin, *Liquid Interfaces in Chemistry and Biology*, John Wiley & Sons, New York, 1998.
- [3] J.E.B. Randall, *Phys. Chem. Liq.* 7 (1977) 107.
- [4] D. Liu, G. Ma, L.M. Levering, H.C. Allen, *J. Phys. Chem. B* 108 (2004) 2252.
- [5] L.M. Levering, M.R. Sierra-Hernández, H.C. Allen, *J. Phys. Chem. C* 111 (2007) 8814.
- [6] B.P. Pettersen, R.J. Saykally, M. Mucha, P. Jungwirth, *J. Phys. Chem. B* 109 (2005) 7976.
- [7] B. Schnell, R. Schurhammer, G. Wipff, *J. Phys. Chem. B* 108 (2004) 2285.
- [8] L. Vrbka, M. Mucha, B. Minofar, P. Jungwirth, E.C. Brown, D.J. Tobias, *Curr. Opin. Colloid Interface Sci.* 9 (2004) 67.
- [9] J.L. Thomas, M. Roeselova, L.X. Dang, D.J. Tobias, *J. Phys. Chem. A* 111 (2007) 3091.
- [10] M. Xu, R. Spinney, H.C. Allen, *J. Phys. Chem. B* 113 (2009) 4102.
- [11] M. Xu, C.Y. Tang, A.M. Jubb, X. Chen, H.C. Allen, *J. Phys. Chem. C* 113 (2009) 2082.
- [12] G.G. Roberts, *Langmuir–Blodgett Films*, Plenum Press, New York, 1990.
- [13] D.K. Schwartz, *Surf. Sci. Rep.* 27 (1997) 241.
- [14] R.S. Ghaskadvi, S. Carr, M. Dennin, *J. Chem. Phys.* 111 (1999) 3675.
- [15] S. Mann, *Science* 365 (1993) 499.
- [16] B. Martín-García, M.M. Velázquez, J.A. Pérez-Hernández, J. Hernández-Toro, *Langmuir* 26 (2010) 14556.
- [17] J.M. Bloch, W. Yun, *Phys. Rev. A* 41 (1990) 844.
- [18] E.M. Knipping, M.J. Lakin, K.L. Foster, P. Jungwirth, D.J. Tobias, R.B. Gerber, D. Dabdub, B.J. Finlayson-Pitts, *Science* 288 (2000) 301.
- [19] A. Laskin, D.J. Gaspar, W. Wang, S.W. Hunt, J.P. Cowin, S.D. Colson, B.J. Finlayson-Pitts, *Science* 301 (2003) 340.
- [20] C.M. McGregor, C. Perrin, M. Monck, P. Camilleri, A.J. Kirby, *J. Am. Chem. Soc.* 123 (2001) 6215.
- [21] K. Esumi, J. Hara, N. Aihara, K. Usui, K. Torigoe, *J. Colloid Interface Sci.* 208 (1998) 578.
- [22] R. Zana, *Adv. Colloid Interface Sci.* 97 (2002) 205.
- [23] Z.X. Li, C.C. Dong, J.B. Wang, R.K. Thomas, J. Penfold, *Langmuir* 18 (2002) 6614.
- [24] X. Chen, J. Wang, N. Shen, Y. Luo, L. Li, M. Liu, R.K. Thomas, *Langmuir* 18 (2002) 6222.
- [25] G. Zhang, X. Zhai, M. Liu, *J. Phys. Chem. B* 110 (2006) 10455.
- [26] Q. Chen, L. Xiaodong, W. Shaolei, X. Shouhong, H. Liu, Y. Hu, *J. Colloid Interface Sci.* 314 (2007) 651.
- [27] R. Li, Q. Chen, D. Zhang, H. Liu, Y. Hu, *J. Colloid Interface Sci.* 327 (2008) 162.
- [28] Q. Chen, D. Zhang, R. Li, H. Liu, Y. Hu, *Thin Solid Films* 516 (2008) 8782.
- [29] R. Zana, M. Benraou, R. Rueff, *Langmuir* 7 (1991) 1072.
- [30] Y. Wang, E.F. Marques, C.M. Pereira, *Thin Solid Films* 516 (2008) 7458.
- [31] G.L.J. Gaines, *Insoluble Monolayers at the Liquid–Gas Interfaces*, Wiley-Interscience, New York, 1966.
- [32] M.C. Gurau, S.-M. Lim, E.T. Castellana, F. Albertorio, S. Kataoka, P.S. Cremer, *J. Am. Chem. Soc.* 126 (2004) 10522.
- [33] A. Aroti, E. Leontidis, E. Maltseva, G. Brezesinski, *J. Phys. Chem. B* 108 (2004) 15238.
- [34] E. Leontidis, A. Aroti, L. Belloni, *J. Phys. Chem. B* 113 (2009) 1447.
- [35] E. Leontidis, A. Aroti, *J. Phys. Chem. B* 113 (2009) 1460.
- [36] F. Hofmeister, *Arch. Exp. Pathol. Pharmacol.* 24 (1888) 247.
- [37] W. Kunz, J. Henle, B.W. Ninham, *Curr. Opin. Colloid Interface Sci.* 9 (2004) 19.
- [38] P.B. Petersen, R.J. Saykally, M. Mucha, P. Jungwirth, *J. Phys. Chem. B* 109 (2005) 10915.
- [39] M. Sovago, G. Wurpel, M. Smits, M. Muller, M. Bonn, *J. Am. Chem. Soc.* (2007) 11079.
- [40] K. Holmer, B. Jönsson, B. Kronberg, B. Lindman (Eds.), *Surfactants and Polymers in Aqueous Solution*, 2nd Ed., Wiley, 2003, p. 61.
- [41] E. Khurana, S.O. Nielsen, M.L. Klein, *J. Phys. Chem. B* 110 (2006) 22136.